Journal of Photochemistry and Photobiology 29 (2025) 100267

Contents lists available at ScienceDirect

Journal of Photochemistry and Photobiology

journal homepage: www.sciencedirect.com/journal/journal-of-photochemistry-and-photobiology

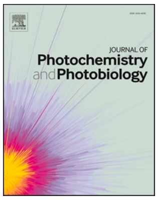

Autologous platelet-rich plasma exosome quantification after two thermo-photobiomodulation protocols with different fluences

Laura Cordero [a], Joan Carles Domingo [b], Elena Sánchez-Vizcaíno Mengual [a,*], Hernán Pinto [a]

[a] *Meta Cell Technology. Sant Cugat, Spain*
[b] *Department of Biochemistry and Molecular Biomedicine, University of Barcelona Faculty of Biology, Barcelona, Spain*

ARTICLE INFO

Keywords:
Platelet-rich plasma
Thermo-photobiomodulation
Temperatures
Exosome
Quantification method
Isolation method
Nanoparticle tracking analysis

ABSTRACT

Objective: The study aimed to assess the effects on exosome quantification of thermo-photobiomodulation (TPBM) with blue light administered at two different fluences for preconditioning platelet-rich plasma (PRP).
Material and Methods: This was an in-vitro study aiming to compare the number of exosomes released from PRP samples after preconditioning for 10 min with blue light (467 nm) at two different fluences, 1.0 J/cm^2 and 2.0 J/cm^2, and controlled heating at 37 °C. PRP samples form three healthy donors were obtained after withdrawing 64 mL of blood and were preconditioned following the two protocols using the MCT System®, a TPBM device with different energy, wavelength, temperature, and time combinations settings. Samples were placed in the MCT Kit® during the procedure, a single-use class IIa device with specific optical properties to optimize light scattering and transmittance. Exosomes were isolated by ultracentrifugation and quantified in triplicate using Nanoparticle Tracking Analysis (NTA).
Results: The mean exosome concentration was 2.99×10^{11} particles/mL (SD 1.31×10^{11}) for the samples exposed to 1.0 J/cm^2 and 2.53×10^{11} particles/mL (SD 1.39×10^{11}) for the samples exposed to 2.0 J/cm^2 ($p = 0.0262$). The lower light fluence resulted in a 15.4 % increase in exosome concentration compared to the highest one.
Conclusions: Different light fluences during the PRP preconditioning resulted in varying exosome concentrations, with the lowest fluence producing the highest yield. Further research is required to determine whether other fluences can improve outcomes and identify the most suitable preconditioning protocol.

1. Introduction

Extracellular vesicles (EVs) are spherical phospholipid bilayer secretory vesicles with sizes ranging from 30 to 2000 nm that are released from almost all cell types [1]. EVs are present in most biological fluids, including bodily fluids such as blood, urine, saliva, breast milk, bronchial lavage, cerebrospinal fluid, and amniotic fluid [2]. Based on their size, biogenesis, compositions, and functions, EVs are classified into three main subgroups: exosomes, microvesicles (MVs), and apoptotic bodies [3].

Exosomes are the smallest EVs, ranging from 30 to 150 nm, and play crucial roles in normal physiological processes and pathological conditions, such as cell signaling [4], immune response [5], or tumor metastasis [1]. They contain bioactive molecules, such as proteins, lipids, and genetic information, including mRNA and noncoding RNAs such as microRNAs (miRNAs) [6], and display other proteins in their membranes [7]. The biogenesis of exosomes entails fusion of intracellular multivesicular bodies (MVBs) with the plasma membrane [8], but the molecular mechanism is still poorly understood [9]. Exosome release depends on several physicochemical factors and cellular conditions, such as lipopolysaccharides, tumor necrosis factor-α, interferon-gamma, hypoxia, calcium, chemotherapeutic drug exposure, and oxidative stress [10,11]. Furthermore, higher temperatures increase the frequency of membrane fusion, accelerating the kinetics of exosome release [12].

Therapeutic applications of exosomes are still in their early stages, and, consequently, the optimal exosome dose for each specific use remains unknown. The optimal dose may depend on the exosome origin, the treatment site, and the intended therapeutic effect. Some studies have suggested that EVs exhibit bimodal dose-dependent effects, whereby EVs may exhibit one effect at specific concentrations while other concentrations may generate opposing effects, implying concentration-dependent effects [13,14]. This model is consistent with the diversity of signaling molecules and pathways associated with EVs

---

* Corresponding author at: Manel Farrés, 101. 08173 Sant Cugat del Vallés, Spain.
E-mail address: esvizcaino@clinipro.net (E. Sánchez-Vizcaíno Mengual).

https://doi.org/10.1016/j.jpap.2025.100267

[15]. For example, a previous study assessing the effects of EVs from platelet-rich plasma (PRP) on cartilage repair in animals showed concentration-dependent effects [16]. Given the importance of determining the optimal dose, the ability to modulate and tailor exosome production could accelerate their development as a therapeutic tool.

Several strategies have been investigated to modulate exosome release, including electrical stimuli, pharmacological agents, electromagnetic waves, sound waves, stress-inducing conditions such as shear stress, cell starvation, acidosis, hypoxia, and inflammation, alcohol, heat, and genetic manipulation [17,18]. However, many of these strategies can alter the properties and biological functions of exosomes, limiting their applicability despite increasing their production. Studies on electromagnetic waves have shown that photobiomodulation with visible light between 455 and 470 nm (blue light) effectively boosts exosome secretion rates from human umbilical cord mesenchymal stem cells (MSCs) [19]. Photobiomodulation uses low-intensity exposure, with intensities ranging from fractions of mW/cm^2 to 100 mW/cm^2, resulting in sample heating typically exceeding 1°C but without causing thermal damage [20,21]. Similarly, photodynamic therapy is associated with hyperthermia [22]. Photobiomodulation conditions leading to heating $\geq$1°C are known as thermo-photobiomodulation (TPBM) and involve a synergistic effect of moderate heating and photobiomodulation [23,24].

In addition to accelerating exosome biogenesis, among other effects, photobiomodulation protects cells from multiple insults and stress conditions, such as inflammatory mechanisms [25], ultraviolet light [26], radiation [27], decreased nutrients, oxidative stress, or lack of oxygen [28,29]. Besides its effects at the cellular level, locally applied photobiomodulation therapy has been shown to enhance tissue healing, reduce pain, and modulate inflammation [30], and may induce systemic effects in approaches such as Intravascular Laser Irradiation of Blood [31]. Although photobiomodulation elicits acute effects, such as analgesia, anti-inflammatory responses, and enhanced mitochondrial activity, its long-term outcomes, including tissue repair, neuroregeneration, and immunomodulation, typically manifest over days to weeks following repeated applications [25,32]. Photobiomodulation induces epigenetic changes that influence gene expression, which may persist throughout multiple cell generations, resulting in long-lasting effects [33].

Despite the advances in TPBM, the optimal wavelength, intensity, and temperature conditions for enhancing exosome release and developing therapeutic products are still under investigation. Moreover, accurately controlling temperature during photobiomodulation may be challenging and requires specific equipment. A TPBM device with temperature control, the MCT System® (Meta Cell Technology, Sant Cugat del Vallès, Spain), was developed to enhance the efficacy of autologous products such as PRP or MSCs, with the potential capability to boost exosome release. The device emits light across a broad wavelength spectrum with simultaneous sample cooling or heating in the range of 4 °C to 45 °C. This study aimed to compare the effects of two different blue light intensities on exosome release from PRP.

2. Material and methods

This was an in-vitro study carried out in the ICMAB-CSIC (Institut de Ciència de Materials de Barcelona) to compare the exosome concentrations released from preconditioned PRP samples from three healthy donors exposed to blue light at two different doses (1.0 J/cm^2 and 2.0 J/cm^2).

2.1. Blood samples collection and processing

Peripheral blood was collected from each donor using a BD Vacutainer Safety-Lok Blood Collection Set 23 g with Pre-Attached Holder 23 g x 178 mm (BD, USA). The 64-mL sample obtained from each donor was equally distributed in eight 3.8 % citrated tubes (8 mL/tube) (Vitrex Medical A/S, Denmark). The tubes were centrifuged at 1800 rpm for 8 min (Steinberg Systems, Germany), yielding approximately 16 mL of PRP.

2.2. Photothermal biomodulation device

The samples were preconditioned with the MCT System (Meta Cell Technology, Sant Cugat del Vallès, Spain), a novel device based on TPBM at controlled temperatures, with specific presets that employ different energy, wavelengths (467 nm, 530 nm, 591 nm, 620 nm, 850 nm), temperature (4°C–45°C), and time (1min–99 min) combinations for preconditioning and priming platelets for promoting the release of platelet-derived exosomes. The MCT System includes the MCT Unit® (Meta Cell Technology, Sant Cugat del Vallès, Spain) and the MCT Kit® (Meta Cell Technology, Sant Cugat del Vallès, Spain), a single-use class IIa medical device that holds the sample during preconditioning.

The MCT Unit® emits continuous light in the range of 467 nm and 850 nm. The MCT Kit® is a 6 × 12-cm medical device that can allocate up to 10 mL of autologous samples. This geometry maximizes the light interface, enabling the optimal exposure of the whole sample. The MCT Kit® 1-mm thick walls are made of a specific medical grade Terlux® polymer modification with the appropriate optical properties to ensure optimal light scattering, transmittance, and other optical properties. A previous study analyzed the optical properties, reporting a 90 % transmittance and <10 % reflectance at wavelengths between 450 nm and 1450 nm [34].

2.3. Preconditioning protocol

All samples were simultaneously exposed to blue light (467 nm) and heated at 37°C at two different light intensities, 1.0 J/cm^2 and 2.0 J/cm^2 during 10 min, to assess the effects of the two light intensities on exosome release. Even though the MCT System allows TPBM at different wavelengths, we used 467 nm light based on previous studies reporting increased exosome yields from MSCs upon exposure to blue light [19].

Each patient sample (16 mL of PRP) was divided into two tubes containing 8 mL each, which were transferred into the MCT Kit® and inserted into the MCT Unit®. Samples from each of the three donors were exposed to the two protocols: blue light (467 nm) at 1.0 J/cm^2 and 37 °C for 10 min, and blue light (467 nm) at 2.0 J/cm^2 and 37 °C for 10 min. Once the conditioning was completed, the kit was retrieved, and the sample was extracted with a syringe and transferred to a 15-mL Falcon tube (Corning, USA) for exosome quantification.

2.4. Exosome quantification by nanoparticle tracking analysis (NTA)

Exosomes were isolated by differential ultracentrifugation, a standard technique that separates EVs from biological fluids based on their size and density through sequential centrifugation steps at increasing speeds. The resulting exosome pellets were resuspended and quantified in triplicate using NTA to assess the effects of two distinct preconditioning blue light doses on exosome release. The NTA measurements were carried out at the ICMAB-CSIC (Institut de Ciència de Materials de Barcelona), an external certified laboratory. Before analysis, samples were diluted (1:1000) in sterile, 0.22 µm-filtered phosphate-buffered saline (PBS) to ensure the particle concentration was within the optimal detection range for NTA, typically between 10^7 and 10^9 particles/mL.

The NTA is based on tracking the motion of individual nanoparticles on a liquid suspension using a laser-illuminated microscope combined with a video camera, allowing calculation of particle size and concentration. We used the Nanosight NS300 instrument (Malvern Panalytical, Salisbury, UK), which analyzes the Brownian motion of nanoparticles in liquid suspension to determine their size and concentration. This technique is based on laser light scattering microscopy combined with video capture, allowing real-time visualization and tracking of individual particles. Particle size is then calculated using the Stokes-Einstein equation, which relates the diffusion coefficient of particles to their hydrodynamic diameter, assuming spherical geometry and known fluid viscosity.

The NanoSight NS300 was equipped with a 488 nm blue laser for particle illumination and a scientific-grade complementary metal-oxide-semiconductor (sCMOS) camera, with high sensitivity and resolution for detecting particles in the exosome size range. For each sample, a 10-second video was recorded at a frame rate of 25.0 frames per second. The video acquisition parameters were optimized for accurate detection, including an exposure level set at 12 for optimal sensitivity, shutter speed slider set at 1200 to control exposure per frame, a gain of 146 to amplify the video signal, and shutter duration of 30 ms. The samples were introduced into the viewing chamber at a constant flow rate using a syringe pump set at 30 arbitrary units (AU), ensuring consistent movement of particles across the field of view.

Each video consisted of 1498 frames and were analyzed with NanoSight software version 3.4 (Build 3.4.4). During data processing, the detection threshold was set at 5, which defines the minimum brightness a particle must exhibit to be recognized. Automatic maximum jump mode was enabled to allow the software to adjust the permitted particle displacement between frames, improving tracking accuracy. Additional parameters included application of a blur filter to reduce background noise, a minimum track length filter to ensure only reliably tracked particles were analyzed, and intensity filters with minimum and maximum values set at 0 and 11,529, respectively, to exclude artifacts and non-specific signals. The particle size estimation was refined using the Finite Track Length Analysis (FTLA) algorithm, which compensates for the limited number of frames over which each particle is tracked. Both the concentration (particles per milliliter) and size distribution (mean, mode, and standard deviation [SD]) of the exosome populations were determined for each sample. Final values were calculated as the mean of three independent measurements.

2.5. Statistical analysis

Quantitative variables were described as the mean and SD. The two light intensity conditions were compared using the *t*-test for two dependent means. The significant threshold was set at $\alpha = 0.05$ ($p < 0.05$).

3. Results

The final quantification conditions for NTA were a mean viscosity of (water) 0.967 mPas and a mean temperature of 21.4 °C.

The concentrations of exosomes upon PRP exposure to the two blue light intensities were significantly different. PRP preconditioning with blue light (467 nm) at 37°C yielded $3.0 \pm 1.3 \times 10^{11}$ particles/mL at 1.0 J/cm^2 intensity and $2.5 \pm 1.4 \times 10^{11}$ particles/mL at 2.0 J/cm^2 intensity ($p = 0.026$) (Table 1 and Fig. 1). Decreasing the blue light intensity from 2.0 J/cm^2 to1.0 J/cm^2 resulted in a 15.4 % increase in exosome concentration. Video 1 and Video 2 of sample 1 are included as an example of the images recorded during the quantification through the NTA method after the PRP sample preconditioning protocol with the MCT System for 10 min, 37 °C, and 1.0 J/cm^2 or 2.0 J/cm^2, respectively.

Table 1
Exosome concentration and size assessments for the two thermo-photobiomodulation settings.

	1 J/cm^2		2 J/cm^2	
Quantification (NTA)	Mean	SD	Mean	SD
Dilution factor*	3.67×10^2	2.31×10^2	3.67×10^2	2.31×10^2
Concentration (EVs /mL)	2.99×10^{11}	1.31×10^{11}	2.53×10^{11}	1.39×10^{11}
Particles per frame	54.5	23.4	42.5	12.4
Centers per frame	60.2	29.2	45.9	14.5
Completed tracks	10,979.6	7676.8	7811.2	3746.0
X-Drift (pix/frame)	−5.1	0.1	−5.2	0.2
Y-Drift (pix/frame)	0.6	0.4	0.6	0.1
Noise level	No			
Size (FTLA)				
Mean (nm)	109.2	5.0	113.4	3.9
Mode (nm)	85.1	10.7	85.3	8.5
SD (nm)	41.6	8.0	43.4	13.5
D10 (nm)	73.0	9.1	75.1	5.8
D50 (nm)	97.3	9.7	101.9	1.8
D90 (nm)	160.9	6.1	167.3	16.3
Valid Tracks	3516.9	1623.0	2938.1	542.6

NTA, Nanoparticle Tracking Analysis; FTLA, Finite Track Length Analysis; EV, extracellular vesicles.
Abbreviations: cm^2, centimeters square; EVs, extracellular vesicles; J, Jules; FTLA, finite track length analysis; nm, nanometers; mL, milliliters; NTA, nanoparticle tracking analysis; SD, standard deviation. Figure Legends.
*Concentrations adjusted for this factor.

4. Discussion

This study assessing the concentrations of exosome released upon preconditioning PRP with the MCT System at two different fluences showed that light intensity applied in the same controlled temperature conditions influenced exosome count. The protocol with the lower fluence (1.0 J/cm^2) yielded significantly higher exosome concentrations than the protocol with 2.0 J/cm^2. This finding raises new questions, and future studies should assess other parameter combinations to determine whether exosome release from PRP can be further boosted.

The number of exosomes can vary depending on the isolation method and quantification techniques, and technical limitations can underestimate or overestimate exosome counts and even impair the functional capacity of exosomes. This study used NTA for the quantification of exosomes, a rapid and highly sensitive method for the visualization and characterization of EVs [35].

Our PRP samples subjected to the TPBM protocols applied with the MCT System obtained a higher exosome concentration than previous approaches based on different agonists to activate PRP [36]. Rui et al. assessed exosome yields from PRP, quantified using nanoflow analysis, and found that activation with saline solution (control) resulted in a mean concentration of 7.52×10^9 particles/mL, whereas activation with calcium gluconate yielded 5.85×10^{10} particles/mL, activation with thrombin yielded 4.87×10^{10} particles/mL, and activation with thrombin and calcium gluconate yielded 7.16×10^{10} particles/mL [36]. Although our results suggest increased exosome release upon TPBM than activation with agonists, the lack of standardized procedures for exosome isolation and quantification precludes direct comparisons between studies.

Studies assessing exosome release from PRP are scarce. Previous studies using other biological materials found that photobiomodulation enhances exosome secretion from dermal papillae, promotes regeneration [37] from endothelial cells [38], and significantly increases EV yield [39], supporting our findings regarding the boosting effects of TPBM on exosome release. Furthermore, another study validated the effects of blue light on boosting angiogenesis, which were attributed to the alterations of miRNAs in exosomes derived from MSCs (MSC-Exo) [19]. However, this previous study did not report exosome concentrations upon blue light photobiomodulation, precluding comparison with this study.

Results from this study should be interpreted in the context of limitations regarding its limited size and conditions assessed. In this regard, this study lacked controls without photobiomodulation and heating, as well as controls with heating alone and photobiomodulation alone, which could have provided baseline values for comparison and help distinguish the individual effects of light and temperature. Furthermore, the absence of reference values for exosome concentration obtained from PRP may limit the interpretation of the results reported in this study. However, this was a proof-of-principle study to assess the effects

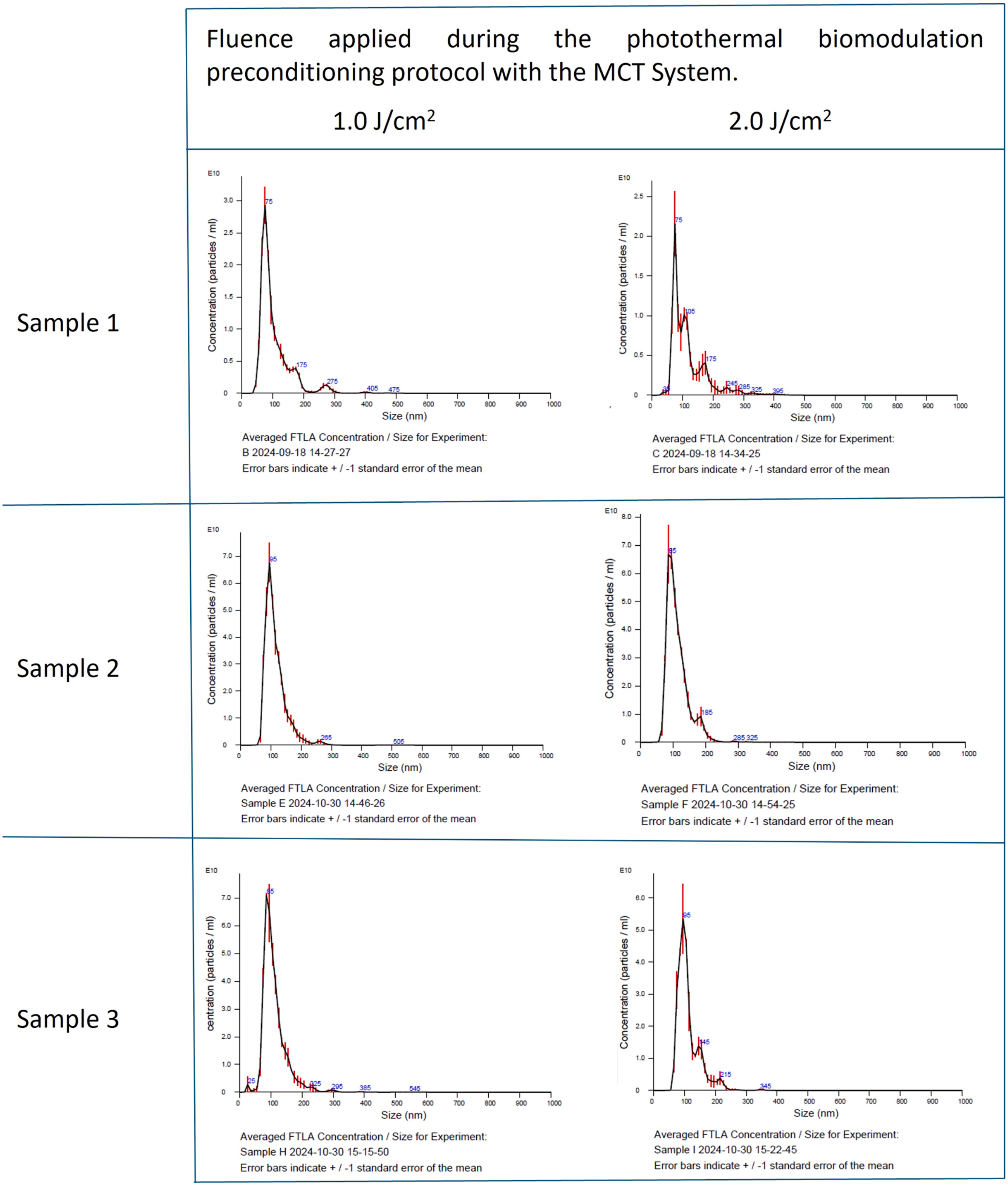

Fluence applied during the photothermal biomodulation preconditioning protocol with the MCT System.

1.0 J/cm²

2.0 J/cm²

Sample 1

Sample 2

Sample 3

Averaged FTLA Concentration / Size for Experiment:
B 2024-09-18 14-27-27
Error bars indicate + / -1 standard error of the mean

Averaged FTLA Concentration / Size for Experiment:
C 2024-09-18 14-34-25
Error bars indicate + / -1 standard error of the mean

Averaged FTLA Concentration / Size for Experiment:
Sample E 2024-10-30 14-46-26
Error bars indicate + / -1 standard error of the mean

Averaged FTLA Concentration / Size for Experiment:
Sample F 2024-10-30 14-54-25
Error bars indicate + / -1 standard error of the mean

Averaged FTLA Concentration / Size for Experiment:
Sample H 2024-10-30 15-15-50
Error bars indicate + / -1 standard error of the mean

Averaged FTLA Concentration / Size for Experiment:
Sample I 2024-10-30 15-22-45
Error bars indicate + / -1 standard error of the mean

Abbreviations: J, Jules; cm², centimeters square; ml, milliliters; nm, nanometers.

Fig. 1. Averaged finite track length analysis (FTLA) concentration/size by sample and preconditioning protocol.

of increasing light fluences on exosome release and provided evidence of decreased exosome concentrations with increased light fluence. Moreover, including more controls may have required an increased number of donors, which was unfeasible given the nature of this study. The effects of different light fluences on the functional properties of exosomes remained unaddressed in this study, which focused on exosome yield. Nevertheless, this study provides valuable insight into the effects of blue light fluences on exosome release with controlled heating. Future, larger studies should expand on combining different wavelengths, fluences, and temperature settings using the MCT System® to determine whether further boosting of exosome release is possible, while preserving exosome function.

5. Conclusions

Preconditioning autologous products used in regenerative medicine is essential to enhance their therapeutic potential and clinical outcomes. The MCT System® is a useful tool that enables clinicians to precondition autologous materials rapidly and safely with a single device. Different blue light fluences for PRP preconditioning resulted in varying exosome concentrations, with the lowest fluence resulting in the highest yield. This study opens multiple avenues for exploring alternative TPBM parameter combinations to identify the most suitable preconditioning protocol for achieving reliable and lasting results in regenerative procedures.

CRediT authorship contribution statement

Laura Cordero: Writing – review & editing, Visualization, Validation, Supervision, Methodology, Conceptualization. **Joan Carles Domingo:** Writing – review & editing, Visualization, Validation, Methodology, Formal analysis, Data curation. **Elena Sánchez-Vizcaíno Mengual:** Writing – review & editing, Writing – original draft, Visualization, Validation. **Hernán Pinto:** Writing – review & editing, Validation, Supervision, Methodology, Conceptualization.

Declaration of competing interest

The authors declare the following financial interests/personal relationships which may be considered as potential competing interests:

Elena Sanchez-Vizcaino Mengual reports a relationship with Meta Cell Technology that includes: employment. Laura Cordero reports a relationship with Meta Cell Technology that includes: employment. Hernan Pinto reports a relationship with Meta Cell Technology that includes: employment. MetaCell Technology paid ICMAB-CSIC (Institut de Ciència de Materials de Barcelona) for the laboratory analyses. Joan Carles Domingo is employed by ICMAB-CSIC; however, he did not receive personal fees. If there are other authors, they declare that they have no known competing financial interests or personal relationships that could have appeared to influence the work reported in this paper.

Acknowledgements

The authors thank the nurses Sandra González and Sonia Jiménez for their assistance in withdrawing blood from the donors. We extend our heartfelt thanks to Dr. Manuel Rubio for providing access to his clinic for the blood extractions and to the entire team at Clínica CIME for their support throughout the process. We sincerely thank Dr. David Ricart Jané from the Department of Biochemistry and Molecular Biology at the University of Barcelona for the coordination of all sample measurements. We are also grateful to José Amable Bernabé from the Institut de Ciència de Materials de Barcelona (ICMAB) for performing our samples' nanoparticle tracking analysis (NTA) measurements. Finally, we would like to acknowledge the generosity of all the donors who contributed their blood, making this study possible.

Funding sources

Meta Cell Technology supported the study.

Supplementary materials

Supplementary material associated with this article can be found, in the online version, at doi:10.1016/j.jpap.2025.100267.

Data availability

The data that support the findings of this study are available from the corresponding author, E.S-V.M., upon reasonable request.

References

[1] F. Momen-Heravi, S.J. Getting, S.A. Moschos, Extracellular vesicles and their nucleic acids for biomarker discovery, Pharmacol. Ther. 192 (2018) 170–187.

[2] K.W. Witwer, E.I. Buzás, L.T. Bemis, et al., Standardization of sample collection, isolation and analysis methods in extracellular vesicle research, J. ExtraCell Vesicles 2 (2013), https://doi.org/10.3402/jev.v2i0.20360. Epub ahead of print 27 January.

[3] L. Doyle, M. Wang, Overview of extracellular vesicles, their origin, composition, purpose, and methods for exosome isolation and analysis, Cells 8 (2019) 727.

[4] C. Corrado, S. Raimondo, A. Chiesi, et al., Exosomes as intercellular signaling organelles involved in health and disease: basic science and clinical applications, Int. J. Mol. Sci 14 (2013) 5338–5366.

[5] A. Bobrie, M. Colombo, G. Raposo, et al., Exosome secretion: molecular mechanisms and roles in immune responses, Traffic 12 (2011) 1659–1668.

[6] R. Kalluri, The biology and function of exosomes in cancer, J. Clin. Investig. 126 (2016) 1208–1215.

[7] N. Palomar-Alonso, M. Lee, M. Kim, Exosomes: membrane-associated proteins, challenges and perspectives, Biochem. Biophys. Rep. 37 (2024) 101599.

[8] M. Xu, J. Ji, D. Jin, et al., The biogenesis and secretion of exosomes and multivesicular bodies (MVBs): intercellular shuttles and implications in human diseases, Genes. Dis 10 (2023) 1894–1907.

[9] G. van Niel, I. Porto-Carreiro, S. Simoes, et al., Exosomes: a common pathway for a specialized function, J. Biochem. 140 (2006) 13–21.

[10] Y.-G. Yuan, J.-L. Wang, Y.-X. Zhang, et al., Biogenesis, composition and potential therapeutic applications of mesenchymal stem cells derived exosomes in various diseases, Int. J. Nanomed. 18 (2023) 3177–3210.

[11] G. Turturici, R. Tinnirello, G. Sconzo, et al., Extracellular membrane vesicles as a mechanism of cell-to-cell communication: advantages and disadvantages, Am. J. Physiol.-Cell Physiol. 306 (2014) C621–C633.

[12] A. Mahmood, Z. Otruba, A.W. Weisgerber, et al., Exosome secretion kinetics are controlled by temperature, Biophys. J. 122 (2023) 1301–1314.

[13] S. Tabak, S. Schreiber-Avissar, E. Beit-Yannai, Extracellular vesicles have variable dose-dependent effects on cultured draining cells in the eye, J. Cell Mol. Med. 22 (2018) 1992–2000.

[14] E.D. Sverdlov, Amedeo Avogadro's cry: what is 1 μg of exosomes? Bioessays 34 (2012) 873–875.

[15] T. Tian, Y. Wang, H. Wang, et al., Visualizing of the cellular uptake and intracellular trafficking of exosomes by live-cell microscopy, J. Cell Biochem. 111 (2010) 488–496.

[16] H. Zhao, Z. Zhao, D. Li, et al., Effect study of exosomes derived from platelet-rich plasma in the treatment of knee cartilage defects in rats, J. Orthop. Surg. Res. 18 (2023) 160.

[17] L. Luo, Z. Wu, Y. Wang, et al., Regulating the production and biological function of small extracellular vesicles: current strategies, applications and prospects, J. Nanobiotechnol. 19 (2021) 422.

[18] N. Erwin, M.F. Serafim, M. He, Enhancing the cellular production of extracellular vesicles for developing therapeutic applications, Pharm. Res. 40 (2023) 833–853.

[19] K. Yang, D. Li, M. Wang, et al., Exposure to blue light stimulates the proangiogenic capability of exosomes derived from human umbilical cord mesenchymal stem cells, Stem Cell Res. Ther. 10 (2019) 358.

[20] E.G. Novoselova, O.V. Glushkova, M.O. Khrenov, et al., Protective effect of low-intensity laser irradiation under acute toxic stress, Biophys. (Oxf) 52 (2007) 83–86.

[21] R. Zein, W. Selting, M.R. Hamblin, Review of light parameters and photobiomodulation efficacy: dive into complexity, J. Biomed. Opt. 23 (2018) 120901.

[22] J. Mattiello, F. Hetzel, L. Vandenheede, Intratumor temperature measurements during photodynamic therapy, Photochem. Photobiol. 46 (1987) 873–879.

[23] R.K. Chailakhyan, A.G. Grosheva, N.N. Vorob'eva, et al., Laser thermo-photobiomodulation of bone marrow mesenchymal stem cells, Bull. Exp. Biol. Med. 174 (2023) 523–526.

[24] J. Kozarev, Concomitant use of autologous exosomes and Nd:YAG laser in post-reconstructive treatment of Bell's palsy: a case report, JPRAS. Open 44 (2025) 199–203.

[25] M.R. Hamblin, M.R. Hamblin, Mechanisms and applications of the anti-inflammatory effects of photobiomodulation, AIMS Biophys. 4 (2017) 337–361. *2017 3:337*.

[26] R. Albarracin, J. Eells, K. Valter, Photobiomodulation protects the retina from light-induced photoreceptor degeneration, Invest. Ophthalmol. Vis. Sci. 52 (2011) 3582–3592.

[27] M. Gobbo, V. Rico, G.N. Marta, et al., Photobiomodulation therapy for the prevention of acute radiation dermatitis: a systematic review and meta-analysis, Support. Care Cancer 31 (2023) 1–14.

[28] A. de Souza da Fonseca, Silva Neto da, L.A. Trajano, E.T.L. Trajano, et al., Effect of low power lasers on prokaryotic and eukaryotic cells under different stress condition: a review of the literature, Lasers. Med. Sci. 36 (2021) 1139–1150.

[29] P. Bikmulina, N. Kosheleva, A. Shpichka, et al., Photobiomodulation in 3D tissue engineering, J. Biomed. Opt. 27 (2022) 090901.

[30] A. Chaple Gil, L. Díaz, A. Von Marttens, et al., The efficacy of low-level laser therapy in oral surgery: a systematic review of randomized controlled trials, Photodiagnosis. Photodyn. Ther. 53 (2025) 104594.

[31] L. Díaz, A.C. Gil, Marttens A Von, et al., The clinical efficacy of intravascular laser irradiation of blood (ILIB): a narrative review of randomized controlled trial, Photodiagnosis. Photodyn. Ther. 53 (2025) 104618.

[32] S. Navarro-Ledesma, A. Gonzalez-Muñoz, J. Carroll, et al., Short- and long-term effects of whole-body photobiomodulation on pain, functionality, tissue quality, central sensitisation and psychological factors in a population suffering from fibromyalgia: protocol for a triple-blinded randomised clinical trial, Ther. Adv. Chronic. Dis. 13 (2022) 1–11.

[33] A.R.N. Zamani, S. Saberianpour, M.H. Geranmayeh, et al., Modulatory effect of photobiomodulation on stem cell epigenetic memory: a highlight on differentiation capacity, Lasers. Med. Sci 35 (2020) 299–306.

[34] H. Pinto, Photoactivation of autologous materials with a new reliable, safe and effective set-up, Aesthet. Med. 6 (2020) 11–15.

[35] N. Comfort, K. Cai, T.R. Bloomquist, et al., Nanoparticle tracking analysis for the quantification and size determination of extracellular vesicles, J. Vis. Exp. (2021), https://doi.org/10.3791/62447. Epub ahead of print 28 March.

[36] S. Rui, Y. Yuan, C. Du, et al., Comparison and investigation of exosomes derived from platelet-rich plasma activated by different agonists, Cell TransPl. 30 (2021), https://doi.org/10.1177/09636897211017833. Epub ahead of print 1 January.

[37] Y. Zhang, J. Su, K. Ma, et al., Photobiomodulation promotes hair regeneration in injured skin by enhancing migration and exosome secretion of dermal papilla cells, Wound Repair Regen. 30 (2022) 245–257.

[38] H.S. Bagheri, M. Mousavi, A. Rezabakhsh, et al., Low-level laser irradiation at a high power intensity increased human endothelial cell exosome secretion via wnt signaling, Lasers. Med. Sci. 33 (2018) 1131–1145.

[39] C.-Y. Chang, A.E. Aviña, C.-J. Chang, et al., Exploring the biphasic dose-response effects of photobiomodulation on the viability, migration, and extracellular vesicle secretion of human adipose mesenchymal stem cells, J. Photochem. Photobiol. B 256 (2024) 112940.